⌘ *Author's Choice*

THE JOURNAL OF BIOLOGICAL CHEMISTRY VOL. 287, NO. 34, pp. 28632–28645, August 17, 2012

Proteomic Analysis of α-Amino-3-hydroxy-5-methyl-4-isoxazole Propionate Receptor Complexes*[S]

Received for publication, December 21, 2011, and in revised form, June 15, 2012 Published, JBC Papers in Press, June 29, 2012, DOI 10.1074/jbc.M111.336644

Myoung-Goo Kang[‡§1], Mutsuo Nuriya[§¶], Yurong Guo[‖], Kevin D. Martindale[‡], Daniel Z. Lee[‡], and Richard L. Huganir[§2]

From the [‡]Department of Neuroscience and Cell Biology, University of Texas Medical Branch, Galveston, Texas 77555, [§]Howard Hughes Medical Institute, Department of Neuroscience, Johns Hopkins University School of Medicine, Baltimore, Maryland 21205, the [¶]Department of Pharmacology, Keio University School of Medicine, 35 Shinanomachi, Shinjuku, Tokyo 160-8582, Japan, and [‖]Susan Taylor Laboratory, University of California San Diego, La Jolla, California 92093

Background: AMPA receptor (AMPA-R) complexes are key players for synaptic transmission and synaptic plasticity.
Results: Optimized proteomic analyses of AMPA-R complexes revealed novel components of AMPA-R complexes.
Conclusion: Optimization of solubilization, enrichment, and immunoprecipitation processes is necessary for AMPA-R complexes proteomics.
Significance: This study contributes to our understanding of synaptic transmission and plasticity and to proteomics of other receptor and ion channel complexes.

The AMPA receptor (AMPA-R) is a major excitatory neurotransmitter receptor in the brain. Identifying and characterizing the neuronal proteins interacting with AMPA-Rs have provided important information about the molecular mechanisms underlying synaptic transmission and plasticity. In this study, to identify more AMPA-R interactors *in vivo*, we performed proteomic analyses of AMPA-R complexes from the brain. AMPA-R complexes were isolated from the brain through various combinations of biochemical techniques for solubilization, enrichment, and immunoprecipitation. Mass spectrometry analyses of these isolated complexes identified several novel components of the AMPA-R complexes as well as some previously identified components. The identification of these novel components helps to further define the complex mechanisms involved in the regulation of AMPA receptor function and synaptic plasticity.

Neurotransmitter-mediated communication between presynaptic and postsynaptic membranes of neurons is the fundamental currency for brain function. The precise organization and dynamic changes of presynaptic and postsynaptic protein components underlie the physiological regulation of synaptic efficacy known as synaptic plasticity. Synaptic plasticity is a central mechanism for the development of the brain and underlies higher cognitive functions of the brain, such as learning and memory. Many studies in neuroscience focusing on the elucidation of the molecular mechanisms of synaptic plasticity have demonstrated the importance of the α-amino-3-hydroxy-5-methyl-4-isoxazole propionate (AMPA) receptors (AMPA-R),[3] the major excitatory neurotransmitter receptor in the brain. The regulation of activity and the trafficking of AMPA-Rs is a potent way of modulating synaptic plasticity underlying many neurobiological functions such as long term potentiation, long term depression, homeostatic synaptic scaling, and learning and memory. Furthermore, the perturbation of synaptic localization of AMPA-R contributes to the pathogenesis of mental retardation, dementia, Alzheimer disease, schizophrenia, and epilepsy (1–4). Therefore, the study of the organization and dynamics of AMPA-R complexes is a key to our understanding of synaptic plasticity, neuronal development, and neurological and psychiatric disorders.

Using a yeast two-hybrid system, several interactors of AMPA-Rs have been identified: GRIP, PICK1, *N*-ethylmaleimide-sensitive factor, protein 4.1 (4.1N), and SAP97 (5–10). The functional study of these previously identified AMPA-R interactors have helped to elucidate mechanisms underlying synaptic plasticity. However, it is likely that there are many more protein-protein interactions that can regulate AMPA-R function and need to be revealed to fully understand how AMPA-Rs regulate synaptic plasticity and brain function.

AMPA-R is a tetramer consisting of a combination of four subunits: GluA1, -2, -3, and -4. Post-translational modifications on these subunits are molecular mechanisms that underlie many types of synaptic plasticity. For example, phosphorylation of AMPA-R subunits is essential for the induction or maintenance of long term depression and long term potentiation (11–15) and learning and memory (16, 17). Palmitoylation of

* This work was supported, in whole or in part, by National Institutes of Health Grants R01NS036715 (to R. L. H.) and N01-HV-28180 (to Y. G.).
⌘ *Author's Choice*—Final version full access.
[S] This article contains supplemental Figs. 1–7.

[1] Supported by an Epilepsy Foundation Postdoctoral Fellowship and start-up fund from University of Texas Medical Branch. To whom correspondence may be addressed: Dept. of Neuroscience and Cell Biology, University of Texas Medical Branch, Galveston, TX 77555-1069. Tel.: 409-772-1186; Fax: 409-762-9382; E-mail: mykang@utmb.edu.
[2] An investigator of the HHMI. To whom correspondence may be addressed: Dept. of Neuroscience, Johns Hopkins University School of Medicine, 725 North Wolfe St., Baltimore, MD 21205. Tel.: 410-955-4050; Fax: 410-955-0877; E-mail: rhuganir@jhmi.edu.

[3] The abbreviations used are: AMPA-R, AMPA receptors; 4.1N, protein 4.1; WGA, wheat germ agglutinin; PSD, postsynaptic density; co-IP, co-immunoprecipitation; IPed, immunoprecipitated; ZO-1, Zonula occludens-1l, NP1, neuronal pentraxin-1; GRP78, 78-kDa glucose-regulated protein; GEF, guanine nucleotide exchange factor.

AMPA-R also plays a critical role for long term depression and long term potentiation (18, 19). Therefore, proteomic analysis of the AMPA-R complexes, which can detect the protein interaction of AMPA-R depending on post-translational modifications, will allow us to identify more AMPA-R interactors that play a role in synaptic plasticity mediated by AMPA-R.

In this study we developed a methodology for proteomic analysis of AMPA-R complexes by combining conventional protein biochemistry and high resolution mass spectrometry. Similar proteomic analyses have been successfully applied to many fields of biological studies, including neuroscience (20–22). Of particular interest, NMDA receptor and calcium channel complexes from the brain were successfully analyzed through proteomic analyses (20, 22).

Here we show the processes of optimizing the conditions for purification of AMPA-R complexes from the brain through combinations of biochemical methodologies adapted from conventional protein biochemistry. The mass spectrometry analyses of these complexes resulted in the identification of several novel interactors of AMPA-R as well as previously identified interacting proteins. We also analyzed the subcellular localization of the three novel interactors to get some mechanistic insights into their potential functions in the brain. Further functional analysis of these novel interactors of AMPA-R will provide a better understanding of the development and function of the brain and may give new insight into neurological and psychiatric disorders.

EXPERIMENTAL PROCEDURES

Preparation of Rat Brain Lysate, Fractionation, and Solubilization—Buffer A was made with a phosphate-buffered saline (PBS: 137 mM NaCl, 2.68 mM KCl, 10.1 mM Na_2HPO_4, 1.76 mM KH_2PO_4, pH 7.4) by freshly adding 0.32 M sucrose, 1 μM microcystine, and protease inhibitor mixture (Complete, Roche Applied Science). Brains were dissected from 3.5-week-old rats (Sprague-Dawley, Harlan, Indianapolis, IN). Several brains (3–7) were used for each experiment. Forebrains, including the cerebral cortex and hippocampus (about 1.0 g together from the 3.5-week-old rat), were used as tissue for immunoprecipitation (IP) with GluA1 antibody. Cerebella were used for IP with GluA4 antibody. The brain tissues were added to Buffer A and homogenized using a glass/Teflon homogenizer. The lysate was centrifuged for 10 min at 1400 $\times$ *g* at 4 °C. The pellet was saved as P1. The supernatant (S1) was collected and spun again at 13,800 $\times$ *g* for 10 min at 4 °C. The second supernatant (S2) and pellet (P2) were saved. The S1, S2, P1, and P2 were either used immediately or stored at −80 °C. Buffer B was made with PBS by freshly adding 0.5% Triton X-100, 0.5 mM EDTA, 0.5 mM EGTA, protease inhibitor mixture, and additional detergents as indicated for each experiment. The P2 was resuspended in Buffer B, mixed gently for 60 min at 4 °C on a rolling platform, and spun down at 14,000 $\times$ *g* for 15 min to collect the supernatant including solubilized proteins.

Purification of AMPA Receptor Complexes—From the solubilized brain P2, matured membrane proteins were enriched through wheat germ agglutinin (WGA) chromatography as described in a previous study (23). Briefly, the solubilized P2 was mixed with WGA (Vector Laboratories, Burlingame, CA) and incubated overnight. After washing with Buffer B, WGA-bound proteins were eluted using *N*-acetyl-D-glucosamine (Sigma). AMPA-R complexes were then purified through medium-scale IP as below.

For this medium scale IP, 100 μg of affinity-purified GluA1 antibody (JH1816) and GluA4 antibody (JH4303) recognizing the N-terminal epitope of GluA1 and GluA4 subunit was used, respectively. Antibodies were bound to Protein A-Sepharose beads (Amersham Biosciences) by incubating at 4 °C for 90 min. To show the specificity of IP, as a negative control, one group of samples was incubated with a synthetic peptide that was used to raise this antibody (peptide block): RH95 for JH1816 and RH258 for JH4303. The solubilized proteins in Buffer B were first incubated with protein A-Sepharose beads for 90 min as a preclearing process and then incubated with the antibody-protein A-Sepharose beads at 4 °C for 3 h on a rolling platform. After washing the beads three times with three-bed volumes of ice-cold Buffer B, proteins bound to the antibodies were eluted with the protein gel loading buffer (2% SDS, 1% β-mercaptoethanol, 0.005% bromphenol blue, 2% glycerol, and 0.05 M Tris-HCl, pH 6.8) and applied to SDS-PAGE (sodium dodecyl sulfate polyacrylamide gel electrophoresis) followed by silver staining and mass spectrometry or Western blot analysis as below. In some cases the AMPA-R complexes bound to the GluA1 antibody were eluted out using the synthetic peptide (RH95) that was used for the development of the GluA1 antibody (JH1816).

SDS-PAGE, Silver Staining, and Peptide Preparation—Immunoprecipitated proteins were resolved by SDS-PAGE using Criterion Precast Gels (Bio-Rad) and stained with Bio-Safe Coomassie stain (Bio-Rad) or Silver Stain Plus™ (Bio-Rad) as per the manufacturer's instruction. Protein bands were excised from the gel in 150-mm Petri dishes and further sliced into ~1 mm cubic pieces. The gel pieces were rinsed with 50% methanol for 10 min twice. For proteins stained with Coomassie Blue, and the gels were re-swollen in 50 μl of 20 mM NH_4HCO_3 for 10 min. After discarding the excess buffer, the gels were dehydrated in 50 μl of CH_3CN for 10 min. For bands stained with silver staining, 30 μl of a 1:1 mix of 30 mM potassium ferricyanide and 100 mM sodium thiosulfate were added to the gel and incubated until the brown color disappeared. The buffer was discarded, and the gel pieces were rinsed with 200 μl of nanopure water. The water was removed, and the gel pieces were rinsed with 100 μl of ammonium bicarbonate (100 mM, pH 8, Sigma). The gel pieces were then lyophilized to dryness in a SpeedVac (ThermoSavant, Holbrook, NY), reduced with DTT (100 μl, 10 mM, pH 8) at 57 °C for 1 h, and alkylated with 100 μl of iodoacetamide (55 mM, pH 8) in the dark at room temperature for 45 min. The supernatant was then removed, and the gel pieces were washed with 100 μl of ammonium bicarbonate (100 mM, pH 8), dehydrated with acetonitrile, and lyophilized to dryness in the SpeedVac. Gels were re-swollen in 50 μl of 20 mM NH_4HCO_3, dehydrated in 100 μl of CH_3CN for 10 min, re-swelled and dehydrated once more, and dried using the SpeedVac. The dried gels were re-swollen in 25 μl of 10 ng/μl trypsin (Sequencing Grade Modified Trypsin, Promega, Madison, WI) in 20 mM NH_4HCO_3 for 60 min on ice. After removing the excess buffer, the gels were covered in 25 μl of 20 mM NH_4HCO_3 and digested at 37 °C overnight. In addition to the

resulting supernatant, the digested peptides were further extracted from the gel once in 25 μl of 20 mM NH_4HCO_3 and 3 times in 50 μl of 50% CH_3CN and 5% formic acid with gentle agitation using vortex each 20 min. All the extracts were combined and dried in the SpeedVac. All tubes and tips used in sample preparations for mass spectrometry were rinsed with CH_3CN before use.

Matrix-assisted Laser Desorption/Ionization (MALDI) and Analysis of Mass Spectrometry Data—After extracted peptides were cleaned using C18 ZipTips (Millipore, Bedford, MA) as per the manufacturer's instruction, 1 μl of peptide samples were mixed with 1 μl of matrix solution (10 mg/ml of α-cyano-4-hydroxycinnamic acid in 50% CH_3CN, 0.3% trifluoroacetic acid) on a 100-well stainless steel target plate (Applied Biosystems, Foster City, CA) by pipetting and air-dried. Spectra of peptides masses were analyzed using Voyager DE-STR MALDI time of flight (TOF) mass spectrometry (MS) (Applied Biosystems) in the reflectron mode. The system was calibrated using the control peptides, and mass spectra of sample peptides were acquired based on this calibration. Obtained spectra were further calibrated by the internal control using the trypsin peptide fragment masses. Peptide peaks were revealed by de-isotoping the spectra, and the masses of the peaks were obtained automatically after setting the threshold to eliminate background signals. Collections of peptide masses were then put into Protein Prospector search engine and analyzed for their matches with peptide mass finger print of reported proteins. Databases were downloaded from EMBL-EBI. These databases were then indexed with trypsin as an enzyme, and maximum 2 internal cleavage sites were allowed. Once a protein was identified with several peptide matches, we made sure either that they belong to rat or that peptide sequences are identical to that of rat.

Liquid Chromatography/Tandem Mass Spectrometry (LC-MS/MS) and Data Base Analysis—LC-MS/MS and data base analysis were performed as described previously (24) with some modifications. Briefly, the extracted and digested peptides were loaded to a reverse-phase C18 precolumn (Shimogyo, Kyoto). The precolumn was connected via Teflon tubing to a C18 analytical column (Waters, Milford, MA) with an integrated emitter tip (2–4-μm inner diameter). Peptides were eluted into a LCQ DECA XP Plus mass spectrometer (ThermoFinnigan, San Jose, CA) with an Agilent 1100 HPLC system. The mass spectrometer was operated in a data-dependent mode in which every MS scan was followed by MS/MS scans on the top five most abundant ions (isolation window = 1.5 Da; dynamic exclusion: repeat count = 1, repeat duration = 0.5 min, duration = 1 min). Protein identification was performed by searching the raw spectra against nr data base using the Bioworks 3.1 software package (Thermo Electron, San Jose, CA) with TurboSequest algorithm. The NCBI nr data base was indexed with trypsin as an enzyme (two internal cleavage sites as maximum). Proteins were accepted only when at least two peptides passed our criteria: ΔCn is above 0.1 and Xcorr values of greater than 3 for triple-, 2.3 for double-, and 2 for single-charged ions. All positively identified peptides were manually confirmed. For positive protein identifications from rat, we made sure that the peptides identified for that protein from nr data base match the peptide sequences from rat.

Western Blot Analysis—Western blot analyses were performed as described previously (11). All antibodies were previously described or were acquired commercially: GluA1-Nt (JH1816), GluA1-Ct (JH4294), GluA2-Ct (MAB397, Chemicon, Temecula, CA), Stargazin (JH3699), GluA2/3 (JH4854), GRIP1 (JH2497), SAP97 (JH4189), GRP78 (PA1-D14, Affinity BioReagent, Golden, CO), 14-3-3 (Santa Cruz Biotechnology, Santa Cruz, CA), *N*-ethylmaleimide-sensitive factor (Santa Cruz), 4.1N (BD Biosciences), PSD95 (K28/43, Millipore), Zizimin1 (C-15, Santa Cruz), Zonula occludens-1 (ZO-1; H-300, Santa Cruz), GluA1 (RH95, Millipore), NeuN (MAB377, Millipore), LARGE (Rbt331 (25), gift from Kevin P. Campbell, University of Iowa), and ERC2 (U5004 (26), gift from Thomas C. Südhof, Stanford University).

Subcellular Fractionation—The P1, S1, S2, and P2 fractions were prepared as described above. To purify presynaptic and postsynaptic proteins, further subcellular fractionation was performed with the P2 as described previously (27). Briefly, after hypo-osmotic lysis of the P2, synaptosomal membrane proteins were purified through a discontinuous sucrose gradient. From the synaptosomal membrane proteins, presynaptic proteins were solubilized with 0.2% Triton X-100. The insolubilized fraction was considered as postsynaptic density (PSD) proteins.

Immunostaining, Microscopy, and Image Analyses—Cortical neuron cultures were prepared, maintained, immuno-stained, and analyzed as previously described (28). Immuno-stained neurons were imaged using a confocal microscopy system based on Nikon A1 with a 60× oil immersion objective. The images were analyzed using ImageJ software (NIH, Bethesda, MD) and NIS-Element software (Nikon). Except one for ERC2, commercial primary antibodies were used for staining: Zizimin1 (Santa Cruz), ZO-1 (Santa Cruz), MAP2 (PCK-554P, Covance), GluA1 (Millipore). All secondary antibodies were purchased from Molecular Probes/Invitrogen.

Co-localization between GluA1 and one of the novel interactors (Zizimin1, ZO-1, or ERC2) was quantified using the co-localization analysis tool in the NIS-Elements software (Nikon). In the analysis, Manders' overlap coefficients were given and used to obtain the co-localization values as percentages between GluA1 and a protein of interest. These values were shown as the mean ± S.E. Images were taken from at least 10 different neurons cultured from at least three different animals. Statistical analyses of the co-localization were done with one-way analysis of variance followed by Tukey's multiple comparison tests, and the probability (p) of 0.05 or less was considered significant. Statistical analyses were performed using SigmaPlot (Version 12, SYSTAT Software).

RESULTS

Initial Optimization of Conditions for the Isolation of AMPA-R Complexes from the Brain—Among several techniques that could be used for isolation of AMPA-R complexes, co-immunoprecipitation (co-IP) was employed in medium scale as this can isolate *in vivo* protein complexes. This technique was successfully used to identify components of the neuronal ion channel complexes in previous studies (20, 22). Before a medium-scale co-IP of the AMPA-R complexes, some pilot

experiments were performed in small scale to determine optimal conditions for the co-IP. Focus was placed on three aspects; 1) choice of antibody, 2) concentration of salt for washing, and 3) detergent conditions. First, two different antibodies raised against GluA1 were tested for co-IP. One was raised against the N terminus of GluA1, which is an extracellular domain, and another was raised against the very C terminus of GluA1 an intracellular domain containing type-I PDZ ligand. As shown in supplemental Fig. 1*A*, both antibodies immunoprecipitated (IPed) GluA1 specifically, and this immunoprecipitation (IP) was blocked by preincubation of the antibodies with the corresponding antigen peptides (peptide block: Pep+). The peptide block was always used as a negative control in our experiments as even a preimmune serum (normal IgG in supplemental Fig. 1*A*) could pull down many proteins non-specifically. Although many proteins were specifically co-IPed with both antibodies of GluA1, more proteins were co-IPed with the anti-GluA1-N terminus antibody. This is likely due to the fact that many of these protein interactions occur through the C terminus of GluA1 and may be blocked by the anti-GluA1 C-terminal antibodies. Therefore, for both GluA1 and GluA4 IP, N-terminal antibodies were used for the medium-scale co-IP.

Second, based on our pilot experiments for optimization of washing stringency in co-IP, the salt concentration in the washing buffer of co-IP was set at 150 mM of NaCl. For example, when the salt concentration in the washing buffer was raised to 500 mM, many weak protein bands specifically co-IPed with 150 mM salt became too weak to be detected in our gel staining (compare supplemental Fig. 1, *A* and *B*). Third, detergent conditions were empirically determined. Out of many kinds of detergent, we decided to use Triton X-100 for two main reasons. Triton X-100 has been used for most of the biochemical analysis of AMPA-R, as it is effective both in extracting AMPA-Rs and keeping protein-protein interactions intact (29). Triton X-100 is also compatible with mass spectrometry in low concentration. Among different concentrations of Triton X-100 tested from 0.1% to 2.0%, the condition was set to 0.5% based on the yield of co-IP and the signal to noise ratio (data not shown).

Analysis of AMPA-R Complexes through MALDI-TOF—Through optimization as described above, a protocol for medium-scale co-IP of AMPA-R was established and used to isolate native AMPA-R complexes from the membrane fraction (P2) of rat cerebral cortex and hippocampus (see details under "Experimental Procedures") considering its enrichment in the forebrain (30). Eluted proteins from the IP were separated by SDS-PAGE and visualized through silver staining (Fig. 1*A*). IP of GluA1 yields multiple protein bands that were specifically co-IPed with GluA1. Among them, a strong protein band that was migrated ~200 kDa was prominent and reproducibly observed. This protein band was apparent even with a stringent washing condition (supplemental Fig. 1*B*), suggesting a strong interaction with GluA1. Therefore, this band was excised, and its peptide fragments were analyzed using a MALDI TOF system followed by a peptide mass profile search. This analysis identified this band as a protein called Zizimin1, a guanine nucleotide exchange factor (GEF) for CDC42 (31) with a high matching score (Fig. 1, *B* and 1*C*).

A similar IP as above was performed with anti-GluA4 antibodies and a P2 membrane fraction of rat cerebellum (Fig. 2*A*) considering high expression of GluA4 in the rat cerebellum (30). Again, IP of GluA4 yields multiple protein bands that were specifically co-IPed with GluA4. Two co-IPed protein bands were observed reproducibly, one at ~200 kDa and the other at ~50 kDa just below the heavy chain of immunoglobulin (Fig. 2*A*). These protein bands were excised from the gel and analyzed through mass spectrometry. MALDI-TOF analyses followed by data base searches with the resulting peptide fragment mass profiles identified the ~200-kDa protein as ZO-1 and the ~50-kDa protein as NP1 (neuronal pentraxin-1). The peptide mass spectra (Fig. 2*B*) and matching of the resulting masses to the data base (Fig. 2*C*) were shown for the NP1 as an example of the MALDI-TOF analysis.

NP1 is a neuronal pentraxin protein that is known to be associated with AMPA-R through clustering with a homologous protein Narp (32). The identification of NP1 as an interactor of AMPA-R in our medium-scale co-IP demonstrated that our proteomic screening methodology has great potential to identify the other AMPA-R associated proteins.

As shown in Figs. 1*A* and 2*A*, there were additional multiple protein bands (*arrowheads*) specifically co-IPed either with GluA1 or GluA4. However, these bands did not produce peptide mass spectra that were sufficient to determine the identity of these proteins convincingly. This could be due to low amounts of co-IPed protein in the bands, low resolution of MALDI-TOF, or contamination from the other proteins in the band. In all of our proteomic analyses, to eliminate peptides from nonspecific protein bindings, gel pieces (same kDa as a specific band) from the negative control lane (Pep +) were also excised and analyzed through mass spectrometry.

Analysis of AMPA-R Complexes through LC-MS/MS—To identify the protein bands (indicated by *arrowheads* in Figs. 1*A* and 2*A*) that specifically co-IPed with GluAs but could not be resolved by MALDI-TOF, we modified our proteomic methodology of AMPA-R complexes as below (summarized in Fig. 7*A*). First, to increase the resolution of mass spectrometry, LC-MS/MS was adopted instead of MALDI-TOF. Despite the high sensitivity of LC-MS/MS, the detection of integral membrane proteins such as ion channels from protein mixture in the lysate of animal tissues has still been challenging due to low abundance and high hydrophobicity of the proteins. Second, to overcome these problems, a lectin-affinity chromatography was introduced as a membrane protein enrichment process before the medium-scale co-IP. As a lectin for the chromatography, WGA was used because WGA binds to various glycoproteins containing sialic acid that is abundant in plasma membrane proteins such as ion channels including AMPA-R, NMDA receptor, and calcium channels. The WGA chromatography was successfully used for enrichment of AMPA-R from the brain during purification of AMPA-R (33, 34). As shown in supplemental Fig. 2, WGA chromatography significantly decreased background in the silver-stained gels and increased the efficiency of GluA IP. Western blot analysis also demonstrated that the introduction of the WGA chromatography significantly increased the enrichment of GluA1, GluA4, and GluN1 (supplemental Fig. 3). On the other hand, cytoplasmic

A

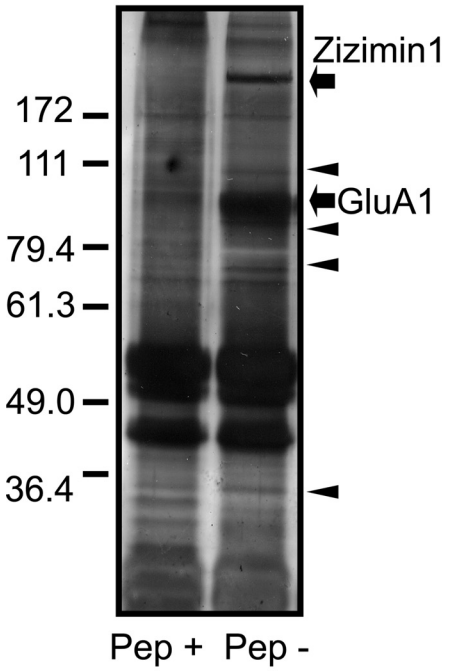

B

	MOWSE Score	#/79(%) Masses Matched	% Cov	% TIC	Mean Err ppm	Data Tol ppm	MS-Digest Index #	Protein MW (Da)/pI	Accession #	Species	Protein Name
1	3.456e+07	24 (30)	14.0	30.4	6.17	35.2	84704	235314/6.9	Q8BIK4	MOUSE	Dedicator of cytokinesis protein 9 (Cdc42 guanine nucleotide exchange factor zizimin 1)
2	2033	12 (15)	5.0	15.2	-5.69	63.7	82652	271066/5.6	Q9QWN8	RAT	Spectrin beta chain, brain 2 (Spectrin, non-erythroid beta chain 2) (Beta-III spectrin) (SPNB-3) (Beta SpIII sigma 1) (Spectrin-like protein GTRAP41)
3	1307	16 (20)	6.0	20.3	-0.332	53.8	91011	340247/5.5	Q60847	MOUSE	Collagen alpha 1(XII) chain precursor
4	468	11 (13)	7.0	13.9	4.47	49.2	109245	142668/6.6	P28818	RAT	Guanine nucleotide releasing protein (GNRP) (P140 Ras-GRF)
5	130	6 (7)	5.0	7.6	0.642	71.8	31695	122575/5.7	P42703	MOUSE	Leukemia inhibitory factor receptor precursor (LIF-R) (D-factor/LIF receptor)

C

1. 24/79 matches (30%).
Acc. #: Q8BIK4 **Species:** MOUSE **Name:** Dedicator of cytokinesis protein 9 (Cdc42 guanine nucleotide exchange factor zizimin 1)
Index: 84704 **MW:** 235314 Da **pI:** 6.9

m/z Submitted	MH^+ Matched	Delta ppm	Modifications	Start	End	Missed Cleavages	Database Sequence
523.1273	523.1319	-8.8	2PO4	333	335	0	(K)STR(E)
568.2665	568.2860	-34	1PO4	887	890	0	(R)VLTR(A)
597.3473	597.3401	12		1049	1053	0	(R)GFVFK (Q)
600.4025	600.4085	-9.9		1151	1155	0	(K)NLLIK (H)
628.1792	628.1785	1.2	2PO4	1750	1753	0	(R)AYSK(V)
711.3910	711.3830	11		1075	1079	0	(K)FEFLR (V)
820.4985	820.4681	37		1460	1466	0	(K)NVFTALR (S)
869.5058	869.4885	20		1764	1770	0	(R)LLGTYFR (V)
949.4862	949.4548	33	1PO4	1764	1770	0	(R)LLGTYFR(V)
949.4862	949.4718	15		532	539	0	(R)MPFAWAAR (T)
1103.5291	1103.4774	47	1PO4	1615	1623	0	(K)SYASTPELR(K)
1149.6080	1149.5904	15		1130	1139	0	(R)EVGTALQEFR (E)
1213.6675	1213.6693	-1.5		1030	1040	0	(K)NANHSLAVFIK (R)
1222.6259	1222.6115	12		522	531	1	(K)QACQRLGQYR (M)
1277.7160	1277.7040	9.4		670	680	1	(K)ARNIAICIEFK (D)
1471.7682	1471.7619	4.3		1504	1515	0	(R)TEASQLLYFLMR (N)
1534.8063	1534.7939	8.1		290	302	0	(K)ILQLNFEAAMQEK (R)
1756.8792	1756.8771	1.2		423	437	0	(K)ISADFHVDLNHFSVR (Q)
1829.9891	1829.9874	0.94		1966	1983	0	(K)LQGSVSVQVNAGPLAYAR (A)
1851.9110	1851.9016	5.0		359	374	0	(K)LDFSSAEPEVKPFEEK (F)
1971.9705	1971.9285	21	1PO4	1945	1961	1	(K)VAELRQLCSSAEVDMIK(L)
1971.9705	1971.9890	-9.4		83	98	0	(R)EMLLFPYDDFQTAILR (R)
2211.1046	2211.0851	8.8	1PO4	758	776	1	(K)DAVETQVGFSWLPLLKDGR(V)
2299.1182	2299.1619	-19		1441	1459	1	(K)VFDVYLCFLQKHQSEMALK (N)
2417.2583	2417.2676	-3.9		1234	1257	0	(K)DLLGAISGIASPYTASTPNINSVR (N)
2706.1890	2706.2309	-15	1PO4	1637	1660	0	(K)NGDLSEAAMCYVHVTALVAEYLTR(K)

FIGURE 1. **Medium-scale immunoprecipitation of AMPA receptor complexes from the forebrain followed by MALDI-TOF analysis.** *A*, shown is silver staining of a 10% protein gel separating proteins that were solubilized with D1 (0.5% Triton X), co-immunoprecipitated with GluA1 antibodies, and eluted with gel loading buffer. *Pep+*, peptide block; *Pep−*, no peptide block. *Arrows* indicate proteins resolved by MALDI-TOF. *Arrowheads* indicate proteins not resolved by MALDI-TOF. *B*, shown are results of the data base search with obtained peptide masses through MALDI-TOF analysis of the ~200-kDa protein band (Zizimin). Zizimin1 is at the top of the list, with the highest score. *C*, shown is a summary of peptide masses matching with the theoretical peptide masses of Zizimin1.

proteins such as GRIP and *N*-ethylmaleimide-sensitive factor were not enriched by WGA chromatography (see Fig. 6, *A* and *D*). Third, to increase the extraction and solubility of AMPA-R, a detergent mixture was used instead of a single detergent. One of the challenges for the proteomic analysis of membrane protein complexes is keeping the integrity of a protein complex without sacrificing extraction efficiency during the solubilization process. The solubilization process could be optimized empirically by trying different kinds of detergents in various concentrations. Of various combinations of detergents, we decided to use two different detergent conditions for the solubilization of AMPA-R from the brain: D1 (0.5% Triton X) or D2 (0.5% Triton X + 0.1% SDS). Finally, to reduce the background in gel caused by nonspecific binding, the elution of AMPA-R co-IPed proteins was performed with synthetic antigenic peptide (elution with peptide) instead of elution with gel loading buffer in some experiments (see Fig. 5, *A* and *B*). By trying various combinations of proteomic screening protocols as described above, we were able to isolate several sets of AMPA-R complex components *in vivo* that could be analyzed through mass spectrometry as shown in our data.

Fig. 3 shows a representative silver staining of protein gel-resolving AMPA-R complexes that was solubilized with D2 from lysate of the forebrain, enriched with WGA chromatography, IPed with anti-GluA1 N-terminal antibody, and eluted with gel loading buffer. Compared with the gel presented in Fig. 1, signal-to-background ratio is much higher due to reduction of nonspecific binding through enrichment process with WGA chromatography. As shown in supplemental Fig. 4, the intensities of these proteins were measured through densitometry scans of each lane of the silver-stained gel using a computer program (Quantity One, Bio-Rad). This densitometry scan was useful to identify protein bands that were difficult to be seen with the naked eye due to neighboring abundant proteins such as GluAs and IgG. The protein bands (indicated by *arrows* or *arrowheads* in Fig. 3*A*) specifically co-IPed with GluA1 were excised and applied to LC-MS/MS analysis. Representative spectra for the analysis of a peptide from Cx_9 band is shown in Fig. 3*C*. As summarized in Fig. 3*B*, LC-MS/MS analysis of these specific bands gave us peptide sequences that are parts of potential AMPA-R interactors. This success is likely due to two major improvements of our proteomic protocol: higher sensi-

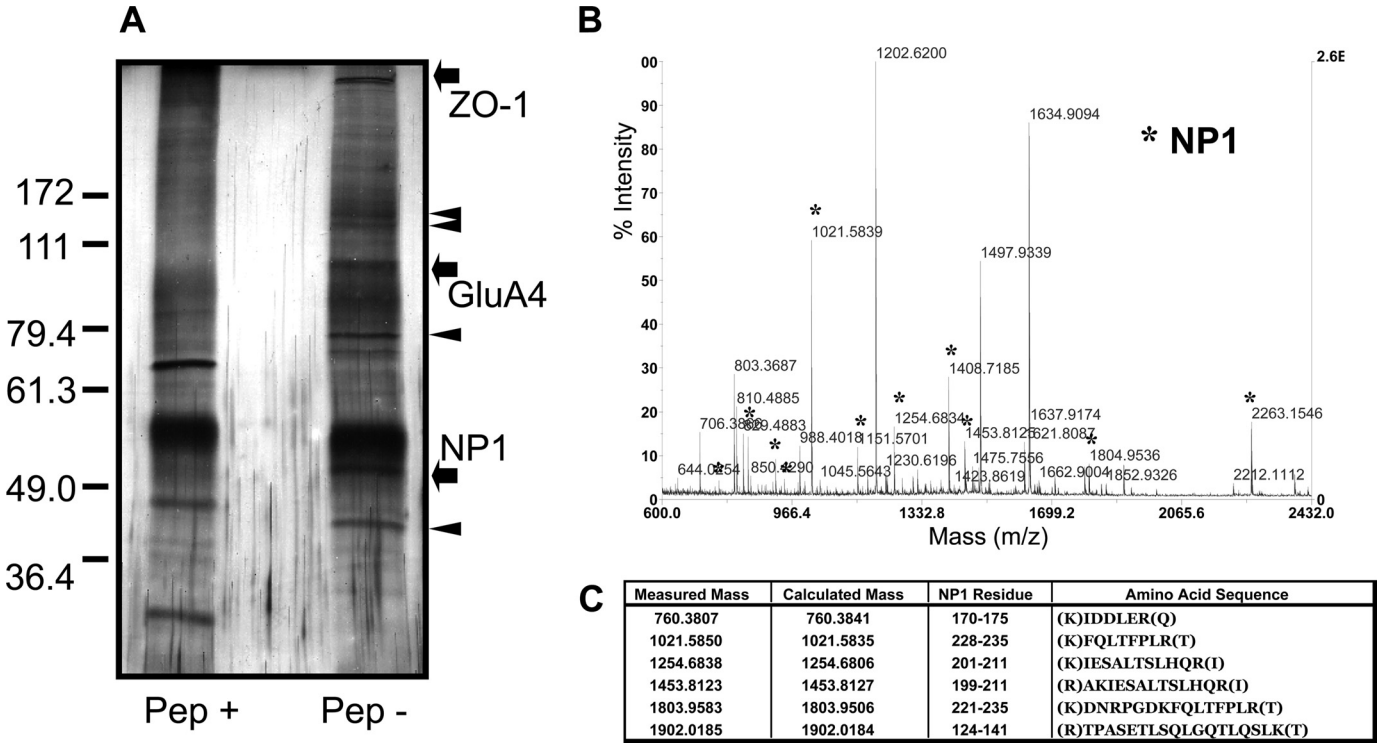

C

Measured Mass	Calculated Mass	NP1 Residue	Amino Acid Sequence
760.3807	760.3841	170-175	(K)IDDLER(Q)
1021.5850	1021.5835	228-235	(K)FQLTFPLR(T)
1254.6838	1254.6806	201-211	(K)IESALTSLHQR(I)
1453.8123	1453.8127	199-211	(R)AKIESALTSLHQR(I)
1803.9583	1803.9506	221-235	(K)DNRPGDKFQLTFPLR(T)
1902.0185	1902.0184	124-141	(R)TPASETLSQLGQTLQSLK(T)

FIGURE 2. **Medium-scale immunoprecipitation of AMPA receptor complexes from the cerebellum followed by MALDI-TOF analysis.** *A*, silver staining of a 10% protein gel separating proteins that were solubilized with D1 (0.5% Triton X), co-immunoprecipitated with GluA4 antibodies, and eluted with gel loading buffer is shown. Legends and symbols are the same as Fig. 1. *B*, shown are the mass spectra of peptides derived from the 50-kDa protein band (NP1). Peaks of peptide masses corresponding to NP1 peptide fragments revealed by the data base analysis are labeled with *asterisks*. *C*, shown is a summary of peptide masses matching with theoretical peptide masses of NP1.

tivity by LC-MS/MS and reduction of nonspecific binding (background in gel) by WGA chromatography. The identity of proteins was double-checked by comparing predicted molecular weights and their migration in the protein gel, which was measured using a computer software (Quantity One, Bio-Rad) as shown in supplemental Fig. 5. As shown in supplemental Fig. 6, peptides identified through LC-MS/MS analysis of the GluA band showed that the coverage and abundance of peptides are consistent with known subunit abundance (GluA1 = GluA2 > GluA3 > GluA4) and interaction with GluA1 (GluA2 > GluA3) in the forebrain (35). This indicates that our proteomic analysis of AMPA-R successfully recapitulates the *in vivo* composition of AMPA-R in the brain. Three bands out of the resolved bands by LC-MS/MS in Fig. 3 were identified as potential components of the AMPA-R complex (supplemental Fig. 7). The Cx_4 band included three peptides that match the sequence of inhibitory subunit 1A of protein phosphatase 1. A previous study suggested that protein phosphatase 1 could modulate AMPA-R possibly through interaction with spinophilin (36). The Cx_9 band included two peptides that match the sequence of adenine nucleotide translocator (ADP/ATP translocase, solute carrier family 25, member 5). This is a novel interactor of AMPA-R. The Cx_11 band included two peptides that match to the sequence of 78-kDa glucose-regulated protein (GRP78). A previous study showed GRP78 could be co-IPed with AMPA-R (37). The specific interaction of GRP78 with GluA1 was also confirmed through Western blot analysis (Fig. 6*C*).

Cerebellar AMPA-R complex was also isolated through the following process: solubilized with D2, enriched with WGA-chromatography, IPed with anti-GluA4 N-terminal antibody, and eluted with gel loading buffer (Fig. 4). LC-MS/MS analysis of protein bands from the cerebellar AMPA-R complex showed two proteins as part of AMPA-R complex. The Bl-4 band included peptides derived from UDP-3–0-acyl *N*-acetylglucosamine deacetylase, which is a novel component of AMPA-R complex in the cerebellum. Bl-11 band included peptides derived from GRP78. This band was exactly the same size protein band as Cx_11 and included the same peptides, indicating that GRP78 is associated with AMPA-R in both the cortex and cerebellum of the brain.

The LC-MS/MS analysis of some protein bands (*e.g.* Cx_2, Cx_6, and Cx_7 in Fig. 3) could not detect peptides except those derived from either GluAs or IgG (supplemental Fig. 7). This could be due to a low percentage of peptides from some proteins compared with that from GluA and IgG. To remove the IgG contamination in these bands, in our medium-scale co-IP, the elution with gel loading buffer was replaced with the elution with peptides. As shown in Fig. 5, the background was significantly reduced by the elution with peptides, demonstrating that the elution with peptides improved the specificity of co-IP. Furthermore, by introducing the elution with peptides, specific peptides from two bands, Cx_6 and Cx_7, could be identified by LC-MS/MS. Fig. 5*C* shows the list of peptides identified from the Cx_6 band. Although there are some peptides from GluA and IgG, many specific peptides for the two proteins were detected (Fig. 5*C*). From the Cx_6 band, two proteins, ERC2 (also known as CAST1) and GEF-H1 (Rho/Rac guanine nucleotide exchange factor 2, also known as Lfc), were identified as

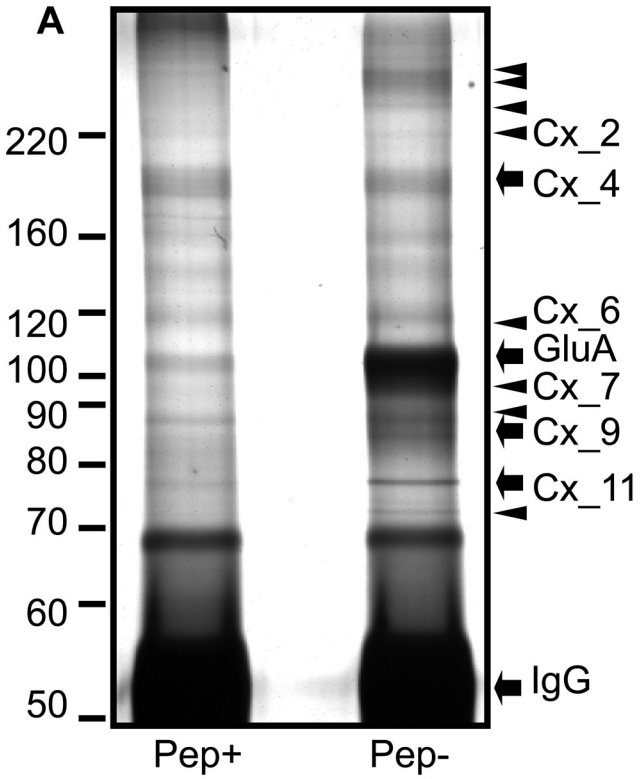

B

Results of LC-MS/MS Analysis

Cx_2: Dimer of GluA1 or IgG heavy chain

Cx_4: Protein Phosphatase 1 Inhibitory subunit 1A

Cx_6: GluA1, IgG

GluA: GluA1, 2, 3, and 4

Cx_7: GluA1, 2, and 3

Cx_9: ADP/ATP translocase (adenine nucleotide translocator) (Solute carrier family 25, member 5)

Cx_11: Heat shock 70kD protein 5 (BiP) (GRP78: 78kDa glucose-regulated protein)

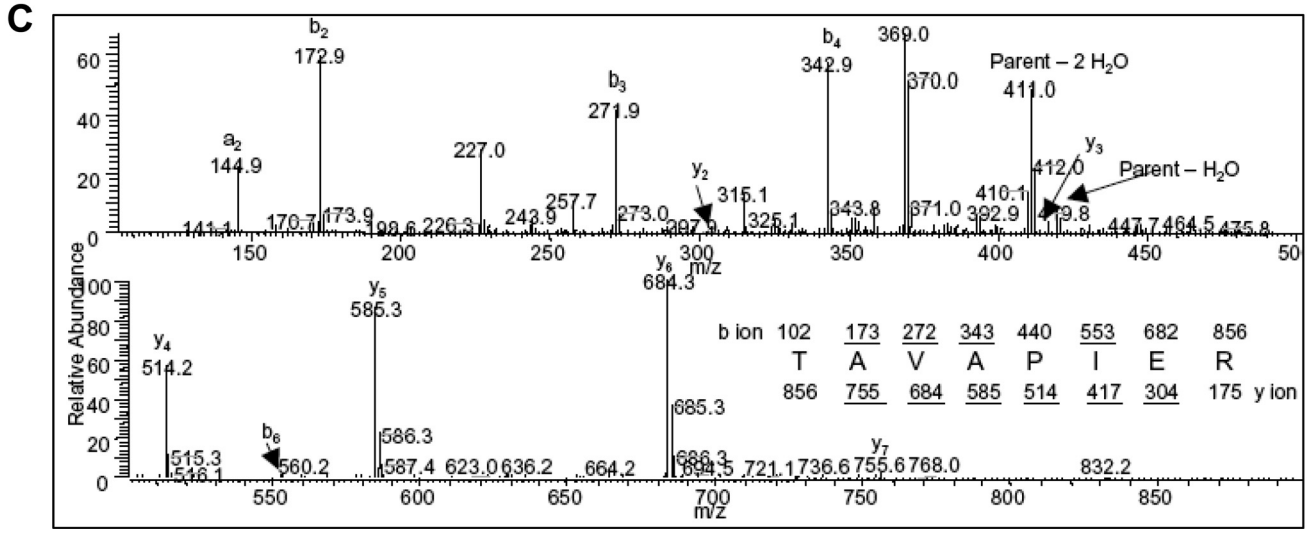

FIGURE 3. **Medium-scale immunoprecipitation of AMPA receptor complexes from the forebrain followed by LC-MS/MS analysis.** *A*, shown is silver staining of a 7.5% protein gel separating proteins that were solubilized with D2 (0.5% Triton X + 0.1% SDS), affinity-purified with WGA-chromatography, co-immunoprecipitated with GluA1 antibodies, and eluted with loading buffer. *Pep+*, peptide block, *Pep−*, no peptide block; *IgG*, immunoglobin G. *Arrows* indicate proteins resolved by LC-MS/MS. *Arrowheads* indicate proteins not resolved by LC-MS/MS. *B*, results of LC-MS/MS analysis followed by a data base search showed a list of proteins specifically co-immunoprecipitated with AMPA-R. *C*, shown are representative LC-MS/MS spectra for the peptide derived from the protein band Cx_9.

novel components of the AMPA-R complex. From the Cx_7 band, LARGE was identified as a novel component of the AMPA-R complex. Our functional analysis of GEF-H1 confirmed GEF-H1 specific interaction with GluA1 and demonstrated that GEF-H1 plays a role for the structural plasticity regulated by AMPA-R activity (28). Our functional analysis of LARGE also suggested that LARGE regulates the trafficking of AMPA-R.[4]

As shown in Fig. 5, by comparing Fig. 5, *A* and *B*, it was noticed that additional detergent decreased the number of proteins that specifically co-IPed with GluA1, presumably due to disruption of protein-protein interactions by adding a stronger detergent. However, some proteins (*e.g.* Cx_7) could be detected in our co-IP only in D2 condition, which could be due to better extraction of AMPA-R from certain membrane (*e.g.* such as PSD).

Eluant of the medium-scale co-IP was also resolved in 5 and 15% SDS-PAGE for better resolution in high and low molecular

[4] M.-G. Kang, unpublished data.

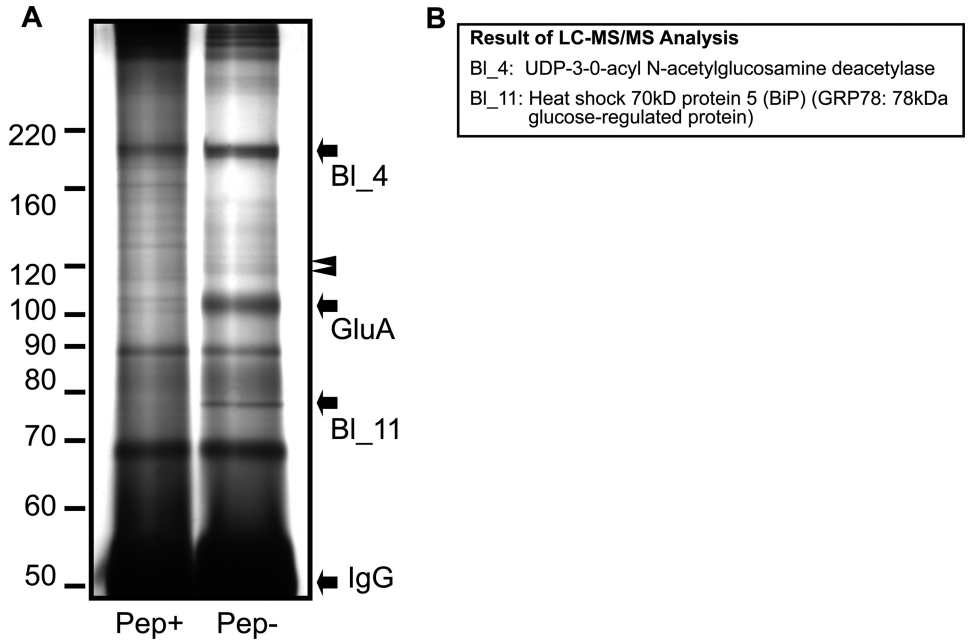

FIGURE 4. **Medium-scale immunoprecipitation of AMPA receptor complexes from the cerebellum followed by LC-MS/MS analysis.** *A*, shown is silver staining of a 7.5% protein gel separating proteins that were solubilized with D2 (0.5% Triton X + 0.1% SDS), affinity-purified with WGA chromatography, co-immunoprecipitated with GluA4 antibodies, and eluted with loading buffer. Legends and symbols are same as Fig. 3. *B*, Results of LC-MS/MS analysis followed by a data base search showed a list of proteins specifically co-immunoprecipitated with AMPA-R.

region, respectively. However, no additional protein bands specifically co-IPed with GluA1 or GluA4 were found.

Western Analysis of AMPA-R Complexes—Western blot analyses with antibodies against known AMPA-R interactors were performed as shown in Fig. 6. GRIP 1 was a part of the AMPA-R complex when the complex was solubilized with D2 but not with D1 solubilization (Fig. 6*A*). SAP97 co-IP was very weak but specific with D1 solubilization (Fig. 6*B*). D2 solubilization caused nonspecific co-IP of SAP97 with GluA1. Western analysis showed that GRP78 was specifically co-IPed with GluA1 with both D1 and D2 solubilization (Fig. 6*C*). The amount of GRP78 co-IPed with GluA1 was very small compared with that in the Input (WGA elute and WGA void in Fig. 6*C*). This could mean that only a small percentage of GRP78 is associated with AMPA-R in the brain. There are two forms (constitutive and inducible forms) of hsp70 in the cerebral cortex and hippocampal synapses (38). The *N*-ethylmaleimide-sensitive factor co-IPed with GluA1 was very weak but specific with both D1 and D2 solubilization (Fig. 6*D*). The Stargazin and γ3 were strongly co-IPed with GluA1 with D1 solubilization but not with D2 solubilization (Fig. 6*E*), suggesting that the additional detergent disrupted the interaction between GluA1 and Stargazin or γ3. The association of 4.1N, PSD95, and LARGE was also confirmed through Western blot analysis as shown in Fig. 6, *F–H*. These proteins were strongly and specifically co-IPed with GluA1. On the other hand, the co-IP of PSD95, 4.1N, and LARGE with GluA4 were difficult to detect in our co-IP. This could be due to relatively low yield of GluA4 co-IP compared with that of GluA1 co-IP.

Immunocytochemical and Biochemical Analyses of Subcellular Localization of Novel Components of AMPA-R Complexes—The protocol and results of our proteomic analyses of AMPA-R complexes were summarized in Fig. 7. To support our proteomic findings, subcellular localization of some novel interactors were analyzed through immuno-staining and subcellular fractionation (Figs. 8 and 9), which could also give us some clues about the potential functions of the novel interactors in the brain as a part of AMPA-R complexes.

Our confocal image analyses showed co-localization of Zizimin1, ZO-1, and ERC2 with GluA1 puncta in the soma, dendrites, and dendritic spines (spines) (Fig. 8, *A* and *B*). Quantification of their co-localization in the dendrites showed that about 20–27% of GluA1 and their puncta were co-localized with each other (Fig. 8*C*). Both in soma and dendrite, Zizimin1 showed bigger puncta compared with those of ZO-1 and ERC2. However, in many cases only a part of the big puncta overlapped with GluA1. ZO-1 puncta in soma were relatively smaller but less diffused compared with those of Zizimin1 and ERC2, suggesting that ZO-1 puncta were arranged in a regular pattern. Our quantification and statistical analyses of the co-localization in the dendrites showed that a significantly higher percentage of GluA1 puncta overlapped with Zizimin1 puncta compared with those overlapping with ZO-1 or ERC2 (Fig. 8*C*), which is consistent to the strong band of Zizimin1 co-IPed with GluA1 (Fig. 1*A*). Some of the partial co-localization of ERC2 puncta with GluA1 puncta showed a typical overlapping feature between a presynaptic and a postsynaptic protein (*double arrowheads* in Fig. 8*A*). Interestingly, more than half of the neurons with ERC2 staining showed nuclear localization of ERC2 (Fig. 8*B*), which was not the case with Zizimin1, ZO-1, and GluA1. The localization of ERC2 in the nucleus observed by immunostaining (Fig. 8*B*) was confirmed through biochemical subcellular fractionation (Fig. 9*A*). ERC2 was enriched in the P1 fraction that included the majority of nuclear proteins as verified by stronger NeuN signal in the P1 fraction compared with that in the other fractions (Fig. 9*A*). Enrichment of all the three

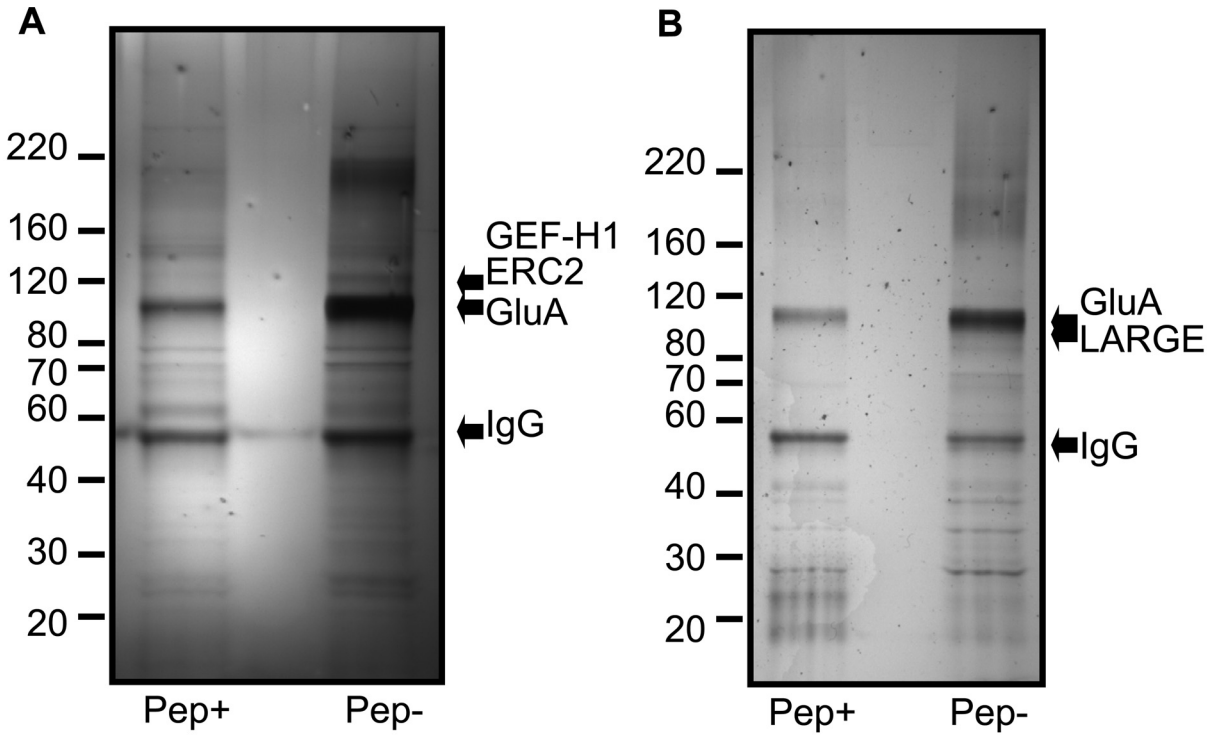

C

Cx_6 Ms/Ms Analysis

#1	**ERC2 (=CAST1) [Rattus norvegicus]**	
	Reference: 23664280	MH+
	-.SLEDDNER.-	977.42
	-.SQLQPEPAK.-	997.53
	-.TISNPEGSPSR.-	1144.56
	-.LASTQQSLAEK.-	1175.63
	-.LGSSMNSIK.-	936.48
#2	**CAST1 (=ERC2) [Rattus norvegicus]**	
	Reference: 22138113	MH+
	-.SLEDDNER.-	977.42
	-.SQLQPEPAK.-	997.53
	-.TISNPEGSPSR.-	1144.56
	-.LASTQQSLAEK.-	1175.63
	-.LGSSMNSIK.-	936.48
#3	Ig gamma H-chain C-region [Oryctolagus cuniculus]	
	Reference: 457366	MH+
	-.NGKAEDNYK.-	1038.49
	-.GQPLEPK.-	768.43
	-.LSVPTSEWQR.-	1202.62
	-.TTPAVLDSDGSYFLYSK.-	1863.90
#4	I46732 Ig gamma heavy chain constant region - rabbit	
	Reference: 2136983	MH+
	-.NGKAEDNYK.-	1038.49
	-.GQPLEPK.-	768.43
	-.LSVPTSEWQR.-	1202.62
	-.TTPAVLDSDGSYFLYSK.-	1863.90
#5	cytomatrix protein p110 [Homo sapiens]	
	Reference: 34577114	MH+
	-.SLEDDNER.-	977.42
	-.SQLQPEPAK.-	997.53
	-.LASTQQSLAEK.-	1175.63
	-.LGSSMNSIK.-	936.48
#6	Unknown (protein for MGC:59433) [Mus musculus]	
	Reference: 34783581	MH+
	-.SLEDDNER.-	977.42
	-.SQLQPEPAK.-	997.53
	-.LASTQQSLAEK.-	1175.63
	-.LGSSMNSIK.-	936.48

#7	KIAA0378porthe grisea 70-15] **(=CAST)**	
	Reference: 20521019, [Homo sapiens]	MH+
	-.SLEDDNER.-	977.42
	-.SQLQPEPAK.-	997.53
	-.LASTQQSLAEK.-	1175.63
	-.LGSSMNSIK.-	936.48
#8	AMPA selective glutamate receptor	
	Reference: 202868	MH+
	-.NSGAGASGGGGSGENGR.-	1391.59
	-.VGGNLDSK.-	789.41
	-.KPCDTMK.-	879.44
#9	**rho/rac guanine nucleotide exchange factor (GEF) 2**	
	Reference: XP_574974, [Rattus norvegicus]	MH+
	-.LRESEQAR.-	988.52
	-.AAVASVTPEK.-	972.54
	-.ATEAGSLEAR.-	1004.50
#10	mKIAA0651 protein [Mus musculus]	
	Reference: 26006191	MH+
	-.LRESEQAR.-	988.52
	-.AAVASVTPEK.-	972.54
	-.ATEAGSLEAR.-	1004.50
#11	similar to Lbcl1 protein [Rattus norvegicus]	
	Reference: 34857950	MH+
	-.LRESEQAR.-	988.52
	-.AAVASVTPEK.-	972.54
	-.ATEAGSLEAR.-	1004.50
#12	**Rho/rac guanine nucleotide exchange factor (GEF) 2**	
	Reference: 13879244, [Mus musculus]	MH+
	-.LRESEQAR.-	988.52
	-.AAVASVTPEK.-	972.54
	-.ATEAGSLEAR.-	1004.50

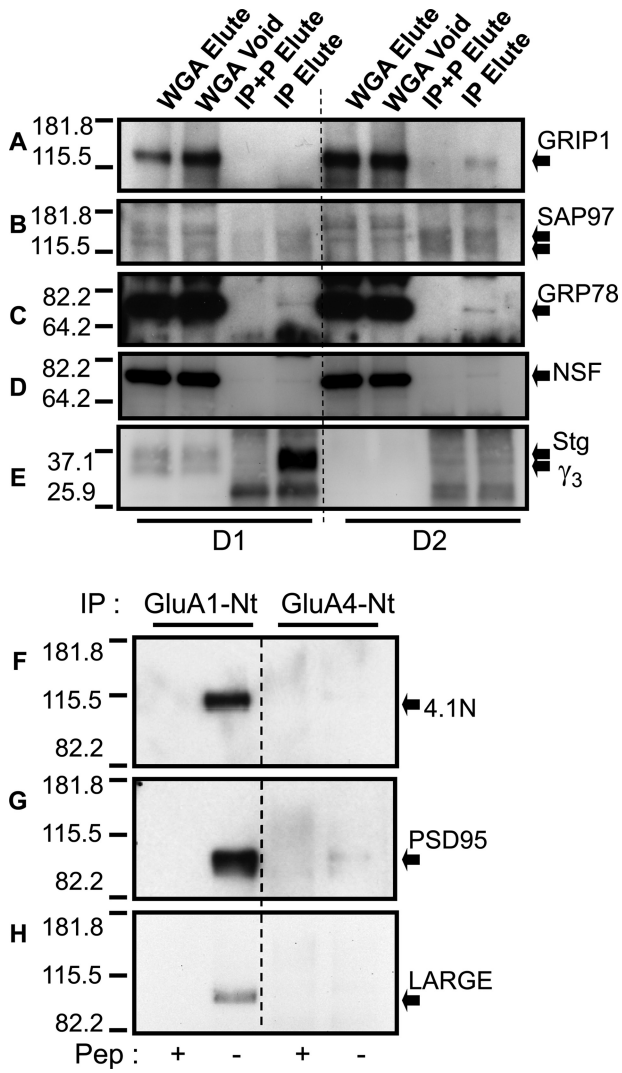

FIGURE 6. **Western blot analysis of AMPA receptor complexes.** *A–E*, samples that were solubilized with either D1 (0.5% Triton X) or D2 (0.5% Triton X + 0.1% SDS) from forebrain lysate, affinity-purified with WGA chromatography (*WGA Elute*), co-IP with GluA1 antibodies, and eluted with gel loading buffer (*IP Elute*) were probed with antibodies against known AMPA-R interactors. *F–H*, Western blots including protein samples that were solubilized with D2 (0.5% Triton X + 0.1% SDS), affinity-purified with WGA chromatography, co-immunoprecipitated with GluA1 or GluA4 antibodies, and eluted with gel loading buffer were probed with antibodies against known or unknown AMPA-R interactors.

in the synaptosomes and PSD (Fig. 9*B*) also supported our hypothesis that the co-localized puncta are in the synapses. Together with our proteomic data, these imaging and subcellular fractionation analyses of novel components suggested their specific interactions with AMPA-R at the synapse.

DISCUSSION

In this study we performed proteomic screening of AMPA-R-associated proteins by combining medium-scale co-IP of

A

1. Solubilization of P2 (from Cortex or Cerebellum) with D1 or D2
2. WGA-affinity chromatography
3. Large-scale co-immunoprecipitation with GluA1 or GluA4 antibodies
   → Elution with loading buffer or Peptide
4. SDS-PAGE → Silver staining
5. Mass spectrometry (MS) analysis of excised protein bands
   MALDI-ToF MS → Peptide mass → Peptide mass fingerprinting
   LC-MS/MS → peptide sequence → NCBI Blast search

B

	GluA1 IP		GluA4 IP	
	D1	D2	D1	D2
Novel	Zizimin1 ERC2/CAST1 GEF-H1/Lfc*	ADP/ATP translocase Phosphatase inhibitor 1 LARGE*	ZO-1	UDP-3-0-acyl N-acetylglucosamine deacetylase
Known		GRP78*	NP1	GRP78

* Double checked by Western Blot analysis

FIGURE 7. **Summary of protocols (*A*) and results (*B*) of proteomic screening of AMPA receptor complexes.** Solubilization condition: D1 (0.5% Triton X), D2 (0.5% Triton X + 0.1% SDS).

AMPA-R and MS. Through this study we developed several methodologies that can isolate sets of components from AMPA-R complexes *in vivo*, resulting in the identification of several novel components of the AMPA-R complex as well as some previously identified AMPA-R interactors (summarized in Fig. 7*B*).

The sensitivity of the LC-MS/MS is high enough to detect a protein even in the femtomolar range. For this high sensitivity, many proteomic analyses using the LC-MS/MS have successfully detected many cytoplasmic proteins even in a small amount of cell lysate. However, proteomic analysis of low abundant integral membrane proteins, such as receptors and ion channels, is still a challenging process for two main reasons: low abundance and high hydrophobicity. In the mixture of proteins from most animal tissues, the relative amount of receptors and ion channels is too low to be detected, as major peptide signals in a mass spectrometry analysis. Isolation of target proteins through the IP process was introduced to overcome this low abundance. However, the IP system should be improved to be compatible with MS because the IP system itself introduces significant contamination through nonspecific binding of proteins as shown in a previous study (22) and our data (Figs. 1–4).

To extract hydrophobic proteins from the membrane, detergents are required but may cause problems in both IP and MS. A successful IP of a membrane protein complex is possible by keeping a balance between extraction efficiency and preservation of protein interactions. Strong detergents (*e.g.* ionic detergent) in high concentrations can extract integral membrane proteins with high efficiency but disrupts protein interactions. To preserve protein interaction during IP, either a low percentage of a strong ionic detergent or a mild non-ionic detergent has

FIGURE 5. **Medium-scale immunoprecipitation of AMPA receptor complexes from the forebrain followed by peptide elution and LC-MS/MS analysis.** *A*, silver staining of a 4–12% gradient protein gel separating proteins that were solubilized with D1 (0.5% Triton X), affinity-purified with WGA chromatography, co-immunoprecipitated with GluA1 antibodies, and eluted with synthetic peptides is shown. This protein gel picture was a part of our previous publication (28). This picture was reused here to compare with other protein gel pictures and to report additional data shown in *C*. *B*, silver staining of a 4–12% gradient protein gel separating proteins that were solubilized with D2 (0.5% Triton X + 0.1% SDS), affinity-purified with WGA chromatography, co-immunoprecipitated with GluA1 antibodies, and eluted with synthetic peptides. Legends and *symbols* are same as Fig. 3, *A* and *B*. *C*, shown is a summary of MS/MS analysis with a protein band Cx_6 that was excised from the protein gel in A. Most of peptide sequences were matched to the sequence of either ERC2/CAST1 (#1, #2, #5, #6, and #7) or GEF-H1 (#9, #10, #11, and #12).

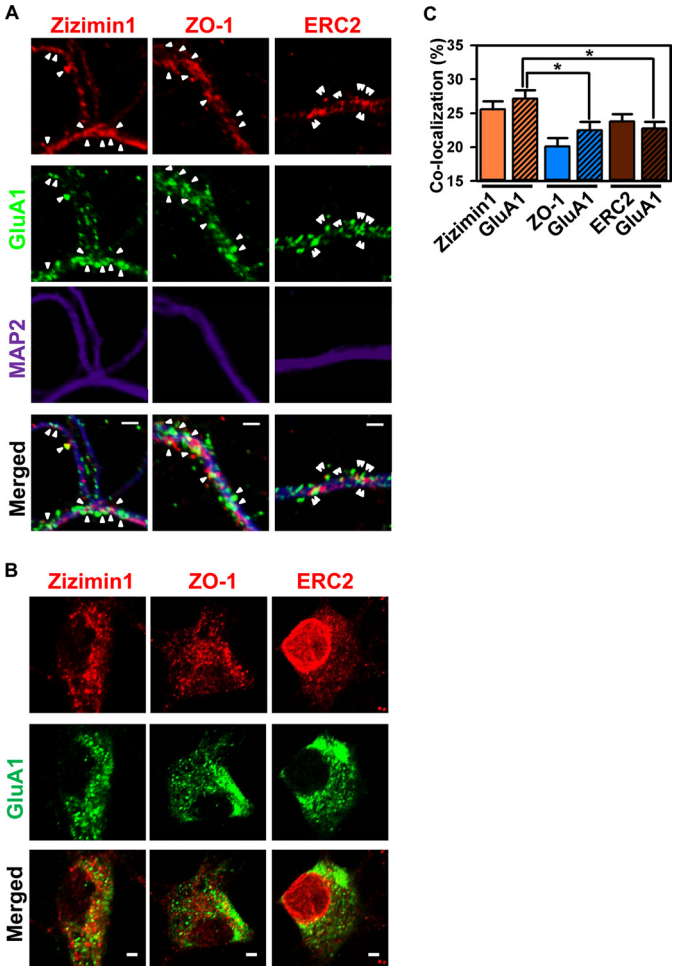

FIGURE 8. **Subcellular localization of three novel components of AMPA receptor complexes in the cultured cortical neurons.** Primary neurons dissociated from cerebral cortex of embryonic age 17 days were cultured for 20–24 days and immunostained with antibodies against the three novel AMPA-R interactors (Zizimin1, ZO-1, and ERC2) and GluA1. *A*, co-localizations of Zizimin1, ZO-1, or ERC2 puncta with GluA1 puncta in the dendrite were labeled with *arrowheads*. *Double arrowheads* indicated partial co-localization of ERC2 puncta with GluA1 puncta that is a typical overlapping feature between a pre-synaptic and a post-synaptic protein. MAP2 was used as a neuronal dendritic marker to show the morphology of the dendrites. *B*, co-localizations of the three proteins with GluA1 in soma is shown. Due to the highly intensive signal of GluA1 and the three proteins in the soma, the gain of their signals in soma were adjusted to a lower level compared with that of dendrites during confocal imaging. All three proteins showed somatic puncta overlap with GluA1 puncta. Significant pools of ERC2 were localized at the nucleus. *Scale bars* are 2 μm (*A* and *B*). *C*, the co-localization of the three proteins with GluA1in the dendrites was analyzed quantitatively by measuring Manders' overlap coefficients that were plotted as the mean ± S.E. The *bars* with diagonal stripes (GluA1) showed percentage (%) of GluA1 puncta overlap with puncta of one of the three proteins. The *bars* with one of the three proteins (Zizimin1, ZO-1, or ERC2) showed % of its puncta overlap with GluA1 puncta. *, $p < 0.05$ ($n = 10$), analysis of variance followed by Tukey's multiple comparison tests.

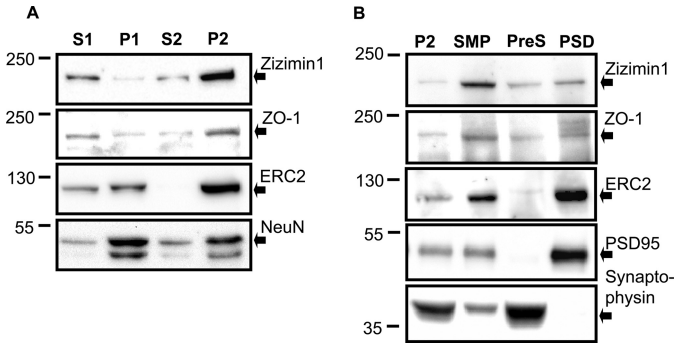

FIGURE 9. **Subcellular localization of three novel components of AMPA receptor complexes in the brain.** Rat brain lysates were fractionated through a series of centrifugation, sucrose gradient, and solubilization. Western blots including protein fractions were probed with antibodies against the three novel AMPA-R interactors. *A*, all three proteins are enriched in the second membrane fraction (*P2*) that mainly includes synaptosomal and mitochondrial membrane proteins. ERC2 is enriched in the first membrane fraction (*P1*) that mainly includes nuclear proteins. NeuN was used as a nuclear protein marker to verify the nuclear protein fraction. *B*, all three proteins are enriched in the synaptosomal membrane protein (*SMP*) and PSD fractions. PSD-95 and synaptophysin were used as pre-synaptic and post-synaptic protein markers, respectively, to verify the pre- and post-synaptic fractionations.

been used for solubilization of membrane protein complexes. In this limited detergent condition, only a small portion of integral membrane proteins was extracted from the membrane.

As shown in a recent study (22) as well as our data (see lane labeled *Pep* + in Figs. 1–4), the major problem of the IP system is nonspecific binding to the IP-matrix, which includes Sepharose/agarose beads, protein A/G, and non-antigen binding sites of antibodies. Preclearing of solubilized brain lysate with protein A-Sepharose beads reduces only a portion of this nonspecific binding. Therefore, in our IP, the nonspecific bindings were always monitored by running a negative control group side-by-side in which synthetic peptides block the binding of antibody to AMPA-R (peptide block, *Pep* + in Figs. 1–5). By analyzing the difference in the protein bands between two groups (Pep + and Pep −), proteins that specifically bind to the antibody can be distinguished from proteins that bind to the IP matrix non-specifically. This peptide block is a more cost-effective negative control compared with the knock-out animal as a negative control.

As a way of overcoming the problems in solubilization and IP as described above, we introduced an enrichment process before IP. In the limited detergent conditions as described above, only a small percentage of integral membrane proteins could be extracted out of the membrane, which was improved by an enrichment process with lectin affinity chromatography. As shown in supplemental Fig. 3, membrane proteins (*e.g.* AMPA-R and NMDA receptor) were effectively enriched using chromatography with WGA. This enrichment process also removed a significant pool of nonspecific protein binding to IP-matrix (supplemental Fig. 2).

Based on our study, it is possible that more than one methodology is necessary for proteomic analysis of AMPA-R complexes. Solubilization with different detergent conditions isolated different AMPA-R complexes. GRIP1 and Stargazin were associated with AMPA-R only in D2 and D1, respectively (Fig. 6, *A* and 6*E*). GEF-H1 and LARGE association with AMPA-R was also detected only in D1 and D2, respectively (Fig. 5). Certain detergent conditions could disrupt some protein interactions in the AMPA-R complex. Different detergents may solubilize different pools of AMPA-R in certain membrane (*e.g.* postsynaptic membrane) that are associated with distinct sets of interacting proteins. In addition, the binding of two proteins to AMPA-R could be competitive *in vivo*. As shown in our data (supplemental Fig. 3), both AMPA-R and NMDA receptors were significantly enriched through WGA chromatography, resulting in the increase in the yield of our proteomic screening

of AMPA-R interactors. However, the association of Zizimin1 with AMPA-R was decreased through the lectin chromatography (compare Figs. 1*A* and 3*A*). Similarly, through the elution with peptides in IP, two additional protein bands (*i.e.* Cx_6 and Cx_7) were resolved by LC-MS/MS. However, due to a low yield of peptide elution, some protein bands were hard to be visualized by silver staining. Therefore, it is possible that only a certain set of components of AMPA-R complex could be isolated through a combination of the proteomic processes. Further optimization of each process in protein sample preparation described above could minimize the numbers of protocols that can cover a wide range of protein interactions in the AMPA-R complex.

Functional studies of the novel components of the AMPA-R complex identified through this study will enhance our understanding of the neurobiological function of the AMPA-R complex. For instance, our functional studies of two of these novel interactors, GEF-H1 and LARGE, have demonstrated important functions of these proteins in structural (28) and functional[4] synaptic plasticity, respectively. Furthermore, through our immunostaining and biochemical studies of Zizimin1, ZO-1, and ERC2 side by side, we analyzed their subcellular localization in the brain and cultured neurons. This could give us insights into their potential function in the brain as well as supportive data for their specific interaction with AMPA-R in the brain and neurons (Figs. 8 and 9).

Zizimin1 is highly expressed in the brain including the hippocampus and cerebral cortex (39). Mediated by its pleckstrin homology and CZH1 domain, Zizimin1 is localization at the membrane (39), which was consistent with our subcellular fractionation data (Fig. 9*A*). Both in soma and dendrite, Zizimin1 puncta were bigger than those of ERC2 and ZO-1 (Fig. 8). In dendrite and soma (Fig. 8), only part of the big puncta or small puncta of Zizimin1 were co-localized with GluA1. However, in spines, Zizimin1 puncta localized throughout almost the entire spine and fully overlapped with GluA1 puncta, although Zizimin1 was not in all spines. Zizimin1 (also known as Dock9) regulates dendrite growth in hippocampal neurons by regulating CDC42 activity (39). Our immunostaining demonstrating Zizimin1 in the spine as well as in the dendrite suggested that Zizimin1 could regulate spine development and/or dynamics. Actually, the developmental profile of Zizimin1 expression in cultured hippocampal neurons demonstrates that its expression is kept high after 13 days *in vitro* (39), when neurons form spines on dendrites (40). Zizimin1 interacts and modulates CDC42 activity to regulate filopodia induction in NIH-3T3 cells (31), suggesting its role in the regulation of actin cytoskeleton dynamics, a key mechanism of spine dynamics (42). GEF-H1, another GEF indentified in our proteomics, regulates spine development depending on AMPA-R activity (28). Together, further analysis of Zizimin1 function in spine development and dynamics is warranted.

Although electron microscopy showed that ERC2 is mainly localized in the active zone (43), ERC2 was originally found in PSD fraction due to its low solubility with mild detergent (*e.g.* Triton X-100) (43). Consistently, in our subcellular fractionation of the brain, ERC2 was enriched not in presynaptic but in PSD fraction (Fig. 9*B*). The low solubility of ERC2 by mild detergents could be due to its tight association with cytoskeletons in the synaptosomal membrane complexes (43). ERC2 is known as a presynaptic scaffolding protein as a member of the active zone-associated structural protein (CAST), which was consistent to our double-staining of ERC2 with GluA1 showing the typical overlapping feature between presynaptic and postsynaptic proteins (*double arrowheads* in Fig. 8*A*). This suggested that ERC2 interacts with AMPA-R through trans-synaptic interaction probably mediated by structural components of synaptic protein complexes. The interaction between ERC2 and AMPA-R could play a role for stabilization of active synapses considering a previous study, the critical role of GluA4 N-terminal region for synaptogenesis (44). In a high percentage of neurons, a significant pool of ERC2 was in the nucleus (Fig. 8*B*). ERC2 was also enriched in P1 fraction, which included nuclear proteins (Fig. 9*A*). A recent study demonstrated that Elongator protein 3 controls active zone morphology by acetylating the Bruchpilot, a member of ELKS/CAST family proteins (45) that includes ERC (46). Given that the Elongator protein 3 orthologs are largely nuclear (45), the nuclear localization of ERC2 is not surprising but actually interesting. Further study of ERC2 subcellular localization could give us a novel insight of ERC2 function in the neurons, such as ERC2 roles in the trafficking of synaptic proteins between cytoplasm and nucleus. ELKS/CAST family proteins have various functions including exocytosis of insulin, microtubule stabilization, and vesicle transport (46).

Although we found ZO-1 as a component of GluA4-containing AMPA-R complexes in the cerebellum, we analyzed ZO-1 in the cerebral cortex and cortical neuron culture as ZO-1 is mainly expressed in the cerebral cortex (mRNA *in situ* images from Allen Institute for Brain Science). In the soma of cultured neurons, ZO-1 was mainly localized in small puncta that seemed to be arranged in a regular pattern (*e.g.* not randomly defused but arranged with regular space). Considering ZO-1 function in intercellular junctions such as tight and adherens junctions (47), the organized pattern of somatic ZO-1 puncta could suggest ZO-1 function in formation and/or regulation of a neuronal junction, the synapse. ZO-1 is a member of the membrane-associated guanylate kinase (MAGUK) homologue family proteins and contains three PSD-95/discs-large/Zonula occludens-1 (PDZ) domains (47), a main protein-protein interaction motif for many synaptic scaffolding proteins, including AMPA-R interacting proteins (41). In our study ZO-1 was enriched in synaptosomal fractions (Fig. 9*B*) and significantly co-localized with GluA1 puncta in neurons (Fig. 8). Thus, ZO-1 might play a role in anchoring AMPA-R in the synapse through its association with AMPA-R complexes.

As described above, the potential functions of these novel interactors of the AMPA-R are very interesting and exciting. Therefore, additional functional studies of these novel interactors will give us a better understanding of the regulation of AMPA-R activity and trafficking and, thus, its role in synaptic transmission and plasticity. Furthermore, these functional studies may significantly contribute to the development of new therapies for the treatment of neurological and psychiatric disorders such as mental retardation, dementia, schizophrenia,

and epilepsy, which are caused by abnormal synaptic transmission and/or plasticity.

REFERENCES

1. Hsieh, H., Boehm, J., Sato, C., Iwatsubo, T., Tomita, T., Sisodia, S., and Malinow, R. (2006) AMPAR removal underlies Aβ-induced synaptic depression and dendritic spine loss. *Neuron* **52,** 831–843
2. Koh, S., Tibayan, F. D., Simpson, J. N., and Jensen, F. E. (2004) NBQX or topiramate treatment after perinatal hypoxia-induced seizures prevents later increases in seizure-induced neuronal injury. *Epilepsia* **45,** 569–575
3. Li, B., Woo, R. S., Mei, L., and Malinow, R. (2007) The neuregulin-1 receptor erbB4 controls glutamatergic synapse maturation and plasticity. *Neuron* **54,** 583–597
4. Pilpel, Y., Kolleker, A., Berberich, S., Ginger, M., Frick, A., Mientjes, E., Oostra, B. A., and Seeburg, P. H. (2009) Synaptic ionotropic glutamate receptors and plasticity are developmentally altered in the CA1 field of Fmr1 knockout mice. *J. Physiol.* **587,** 787–804
5. Dong, H., O'Brien, R. J., Fung, E. T., Lanahan, A. A., Worley, P. F., and Huganir, R. L. (1997) GRIP. A synaptic PDZ domain-containing protein that interacts with AMPA receptors. *Nature* **386,** 279–284
6. Nishimune, A., Isaac, J. T., Molnar, E., Noel, J., Nash, S. R., Tagaya, M., Collingridge, G. L., Nakanishi, S., and Henley, J. M. (1998) NSF binding to GluR2 regulates synaptic transmission. *Neuron* **21,** 87–97
7. Osten, P., Srivastava, S., Inman, G. J., Vilim, F. S., Khatri, L., Lee, L. M., States, B. A., Einheber, S., Milner, T. A., Hanson, P. I., and Ziff, E. B. (1998) The AMPA receptor GluR2 C terminus can mediate a reversible, ATP-dependent interaction with NSF and α-and β-SNAPs. *Neuron* **21,** 99–110
8. Shen, L., Liang, F., Walensky, L. D., and Huganir, R. L. (2000) Regulation of AMPA receptor GluR1 subunit surface expression by a 4.1N-linked actin cytoskeletal association. *J. Neurosci.* **20,** 7932–7940
9. Song, I., Kamboj, S., Xia, J., Dong, H., Liao, D., and Huganir, R. L. (1998) Interaction of the *N*-ethylmaleimide-sensitive factor with AMPA receptors. *Neuron* **21,** 393–400
10. Xia, J., Zhang, X., Staudinger, J., and Huganir, R. L. (1999) Clustering of AMPA receptors by the synaptic PDZ domain-containing protein PICK1. *Neuron* **22,** 179–187
11. Boehm, J., Kang, M. G., Johnson, R. C., Esteban, J., Huganir, R. L., and Malinow, R. (2006) Synaptic incorporation of AMPA receptors during LTP is controlled by a PKC phosphorylation site on GluR1. *Neuron* **51,** 213–225
12. Chung, H. J., Steinberg, J. P., Huganir, R. L., and Linden, D. J. (2003) Requirement of AMPA receptor GluR2 phosphorylation for cerebellar long term depression. *Science* **300,** 1751–1755
13. Lee, H. K., Barbarosie, M., Kameyama, K., Bear, M. F., and Huganir, R. L. (2000) Regulation of distinct AMPA receptor phosphorylation sites during bidirectional synaptic plasticity. *Nature* **405,** 955–959
14. Lee, H. K., Kameyama, K., Huganir, R. L., and Bear, M. F. (1998) NMDA induces long term synaptic depression and dephosphorylation of the GluR1 subunit of AMPA receptors in hippocampus. *Neuron* **21,** 1151–1162
15. Steinberg, J. P., Takamiya, K., Shen, Y., Xia, J., Rubio, M. E., Yu, S., Jin, W., Thomas, G. M., Linden, D. J., and Huganir, R. L. (2006) Targeted *in vivo* mutations of the AMPA receptor subunit GluR2 and its interacting protein PICK1 eliminate cerebellar long term depression. *Neuron* **49,** 845–860
16. Hu, H., Real, E., Takamiya, K., Kang, M. G., Ledoux, J., Huganir, R. L., and Malinow, R. (2007) Emotion enhances learning via norepinephrine regulation of AMPA receptor trafficking. *Cell* **131,** 160–173
17. Lee, H. K., Takamiya, K., Han, J. S., Man, H., Kim, C. H., Rumbaugh, G., Yu, S., Ding, L., He, C., Petralia, R. S., Wenthold, R. J., Gallagher, M., and Huganir, R. L. (2003) Phosphorylation of the AMPA receptor GluR1 subunit is required for synaptic plasticity and retention of spatial memory. *Cell* **112,** 631–643
18. Lin, D. T., Makino, Y., Sharma, K., Hayashi, T., Neve, R., Takamiya, K., and Huganir, R. L. (2009) Regulation of AMPA receptor extrasynaptic insertion by 4.1N, phosphorylation, and palmitoylation. *Nat. Neurosci.* **12,** 879–887
19. Hayashi, T., Rumbaugh, G., and Huganir, R. L. (2005) Differential regulation of AMPA receptor subunit trafficking by palmitoylation of two distinct sites. *Neuron* **47,** 709–723
20. Husi, H., Ward, M. A., Choudhary, J. S., Blackstock, W. P., and Grant, S. G. (2000) Proteomic analysis of NMDA receptor-adhesion protein signaling complexes. *Nat. Neurosci.* **3,** 661–669
21. Peng, J., Kim, M. J., Cheng, D., Duong, D. M., Gygi, S. P., and Sheng, M. (2004) Semiquantitative proteomic analysis of rat forebrain postsynaptic density fractions by mass spectrometry. *J. Biol. Chem.* **279,** 21003–21011
22. Müller, C. S., Haupt, A., Bildl, W., Schindler, J., Knaus, H. G., Meissner, M., Rammner, B., Striessnig, J., Flockerzi, V., Fakler, B., and Schulte, U. (2010) Quantitative proteomics of the Cav2 channel nano-environments in the mammalian brain. *Proc. Natl. Acad. Sci. U.S.A.* **107,** 14950–14957
23. Kang, M. G., Chen, C. C., Felix, R., Letts, V. A., Frankel, W. N., Mori, Y., and Campbell, K. P. (2001) Biochemical and biophysical evidence for γ2 subunit association with neuronal voltage-activated Ca^{2+} channels. *J. Biol. Chem.* **276,** 32917–32924
24. Guo, Y., Ma, S. F., Grigoryev, D., Van Eyk, J., and Garcia, J. G. (2005) 1-DE MS and 2-D LC-MS analysis of the mouse bronchoalveolar lavage proteome. *Proteomics* **5,** 4608–4624
25. Kanagawa, M., Saito, F., Kunz, S., Yoshida-Moriguchi, T., Barresi, R., Kobayashi, Y. M., Muschler, J., Dumanski, J. P., Michele, D. E., Oldstone, M. B., and Campbell, K. P. (2004) Molecular recognition by LARGE is essential for expression of functional dystroglycan. *Cell* **117,** 953–964
26. Wang, Y., Liu, X., Biederer, T., and Südhof, T. C. (2002) A family of RIM-binding proteins regulated by alternative splicing. Implications for the genesis of synaptic active zones. *Proc. Natl. Acad. Sci. U.S.A.* **99,** 14464–14469
27. Kang, M. G., Chen, C. C., Wakamori, M., Hara, Y., Mori, Y., and Campbell, K. P. (2006) A functional AMPA receptor-calcium channel complex in the postsynaptic membrane. *Proc. Natl. Acad. Sci. U.S.A.* **103,** 5561–5566
28. Kang, M. G., Guo, Y., and Huganir, R. L. (2009) AMPA receptor and GEF-H1/Lfc complex regulates dendritic spine development through RhoA signaling cascade. *Proc. Natl. Acad. Sci. U.S.A.* **106,** 3549–3554
29. Blackstone, C. D., Moss, S. J., Martin, L. J., Levey, A. I., Price, D. L., and Huganir, R. L. (1992) Biochemical characterization and localization of a non-*N*-methyl-D-aspartate glutamate receptor in rat brain. *J. Neurochem.* **58,** 1118–1126
30. Martin, L. J., Blackstone, C. D., Levey, A. I., Huganir, R. L., and Price, D. L. (1993) AMPA glutamate receptor subunits are differentially distributed in rat brain. *Neuroscience* **53,** 327–358
31. Meller, N., Irani-Tehrani, M., Kiosses, W. B., Del Pozo, M. A., and Schwartz, M. A. (2002) Zizimin1, a novel Cdc42 activator, reveals a new GEF domain for Rho proteins. *Nat. Cell Biol.* **4,** 639–647
32. Xu, D., Hopf, C., Reddy, R., Cho, R. W., Guo, L., Lanahan, A., Petralia, R. S., Wenthold, R. J., O'Brien, R. J., and Worley, P. (2003) Narp and NP1 form heterocomplexes that function in developmental and activity-dependent synaptic plasticity. *Neuron* **39,** 513–528
33. Chang, Y. C., Wu, T. Y., Li, B. F., Gao, L. H., Liu, C. I., and Wu, C. L. (1996) Purification and biochemical characterization of α-amino-3-hydroxy-5-methyl-4-isoxazolepropionic acid/kainate-sensitive L-glutamate receptors of pig brain. *Biochem. J.* **319,** 49–57
34. Clark, R. A., Gurd, J. W., Bissoon, N., Tricaud, N., Molnar, E., Zamze, S. E., Dwek, R. A., McIlhinney, R. A., and Wing, D. R. (1998) Identification of lectin-purified neural glycoproteins, GPs 180, 116, and 110, with NMDA and AMPA receptor subunits. Conservation of glycosylation at the synapse. *J. Neurochem.* **70,** 2594–2605
35. Wenthold, R. J., Petralia, R. S., Blahos, J., II, and Niedzielski, A. S. (1996) Evidence for multiple AMPA receptor complexes in hippocampal CA1/CA2 neurons. *J. Neurosci.* **16,** 1982–1989
36. Yan, Z., Hsieh-Wilson, L., Feng, J., Tomizawa, K., Allen, P. B., Fienberg, A. A., Nairn, A. C., and Greengard, P. (1999) Protein phosphatase 1 modulation of neostriatal AMPA channels. Regulation by DARPP-32 and spinophilin. *Nat. Neurosci.* **2,** 13–17
37. Rubio, M. E., and Wenthold, R. J. (1999) Calnexin and the immunoglobulin binding protein (BiP) coimmunoprecipitate with AMPA receptors. *J. Neurochem.* **73,** 942–948

38. Moon, I. S., Park, I. S., Schenker, L. T., Kennedy, M. B., Moon, J. I., and Jin, I. (2001) Presence of both constitutive and inducible forms of heat shock protein 70 in the cerebral cortex and hippocampal synapses. *Cereb. Cortex* **11,** 238–248
39. Kuramoto, K., Negishi, M., and Katoh, H. (2009) Regulation of dendrite growth by the Cdc42 activator Zizimin1/Dock9 in hippocampal neurons. *J. Neurosci. Res.* **87,** 1794–1805
40. Wiens, K. M., Lin, H., and Liao, D. (2005) Rac1 induces the clustering of AMPA receptors during spinogenesis. *J. Neurosci.* **25,** 10627–10636
41. Shepherd, J. D., and Huganir, R. L. (2007) The cell biology of synaptic plasticity. AMPA receptor trafficking. *Annu. Rev. Cell Dev. Biol.* **23,** 613–643
42. Cingolani, L. A., and Goda, Y. (2008) Actin in action. the interplay between the actin cytoskeleton and synaptic efficacy. *Nat. Rev. Neurosci.* **9,** 344–356
43. Ohtsuka, T., Takao-Rikitsu, E., Inoue, E., Inoue, M., Takeuchi, M., Matsubara, K., Deguchi-Tawarada, M., Satoh, K., Morimoto, K., Nakanishi, H., and Takai, Y. (2002) Cast. A novel protein of the cytomatrix at the active zone of synapses that forms a ternary complex with RIM1 and munc13–1. *J. Cell Biol.* **158,** 577–590
44. Sia, G. M., Béïque, J. C., Rumbaugh, G., Cho, R., Worley, P. F., and Huganir, R. L. (2007) Interaction of the N-terminal domain of the AMPA receptor GluR4 subunit with the neuronal pentraxin NP1 mediates GluR4 synaptic recruitment. *Neuron* **55,** 87–102
45. Mikiewicz, K., Jose, L. E., Bento-Abreu, A., Fislage, M., Taes, I., Kasprowicz, J., Swerts, J., Sigrist, S., Versées, W., Robberecht, W., and Verstreken, P. (2011) ELP3 controls active zone morphology by acetylating the ELKS family member Bruchpilot. *Neuron* **72,** 776–788
46. Hida, Y., and Ohtsuka, T. (2010) CAST and ELKS proteins. Structural and functional determinants of the presynaptic active zone. *J. Biochem.* **148,** 131–137
47. Fanning, A. S., and Anderson, J. M. (2009) Zonula occludens-1 and -2 are cytosolic scaffolds that regulate the assembly of cellular junctions. *Ann. N.Y. Acad. Sci.* **1165,** 113–120